Morpholine–Phthalocyanine (Donor–Acceptor) Construct: Photoinduced Intramolecular Electron Transfer and Triplet Formation from its Charge Separation State

2 AUTHORS, INCLUDING:

Xian-Fu Zhang
Institute of applied photochemistry, Hebei P…

76 PUBLICATIONS   **714** CITATIONS

SEE PROFILE

Morpholine-Phthalocyanine (Donor−Acceptor) Construct: Photoinduced Intramolecular Electron Transfer and Triplet Formation from its Charge Separation State

Xian-Fu Zhang[*,†,‡] and Jing Wang[†]

[†]Chemistry Department, Hebei Normal University of Science and Technology, Qinghuangdao, Hebei Province, China 066004
[‡]MPC Technology, Hamilton, ON, Canada L8S 3H4

ABSTRACT: Silicon phthalocyanine (SiPc) with two axially attached morpholine (MP) units was prepared, and its photophysics was studied by laser flash photolysis, steady state and time-resolved fluorescence methods. Both the fluorescence efficiency and lifetime of SiPc moiety were remarkably quenched, because of the efficient intramolecular photoinduced electron transfer (PET) from morpholine donors to SiPc moiety. The generated charge separation state (CSS), $SiPc^{\bullet-}-MP^{\bullet+}$, which was observed by transient absorption spectra, showed a lifetime of 4.8 ns. The triplet quantum yield of SiPc unit in the supramolecule is unexpectedly high, and the predominant spectral signal in microsecond-scale is triplet−triplet (T_1-T_n) absorption. This high triplet yield is due to the charge recombination of CSS that generates T_1 in 32% efficiency: $SiPc^{\bullet-}-MP^{\bullet+} \rightarrow {}^3SiPc-MP$. The T_1 formation process occurred efficiently because the CSS $SiPc^{\bullet-}-MP^{\bullet+}$ has a higher energy (1.65 eV) than that of the triplet state ${}^3SiPc-MP$ (1.0 eV). Emission from the CSS was also observed: $SiPc^{\bullet-}-MP^{\bullet+} \rightarrow SiPc-MP + h\nu'$.
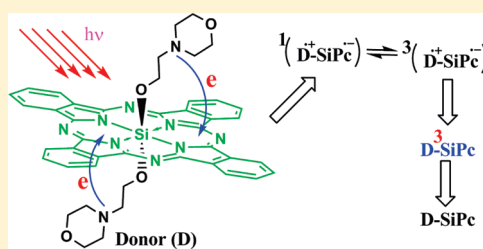
INTRODUCTION

Earth is continuously provided by the Sun with a huge amount of energy, which is fairly distributed all over the world as a clean, abundant, renewable, and economical source. It is, however, cannot be exploited unless it is converted into useful forms of energy for human being.[1,2] Mimicry of photosynthesis in nature has been an actively pursued strategy to this purpose as early as the chemical and biological structure of photosynthetic reaction center was illustrated by X-ray diffraction.[3,4] A large number of artificial constructs being able to undergo intramolecular photoinduced electron transfer (PET),[5] in which either covalent or noncovalent bonding is employed to link a donor (D) and an acceptor (A), have been reported to understand the process of PET, increase PET efficiency and retard charge recombination (CR). Great knowledge has been gained via these investigations: such as the dependence of PET rate constant on driving force (ΔG), medium property, the nature of spacer, the distance and orientation between D and A, etc.[6]

The main focus in artificial photosynthesis has been the obtaining of long-lived charge separation state (CSS). In natural photosynthesis of Photosystem I (PS I), PET proceeds from the excited primary electron donor P700 (a chlorophyll a dimer) via the primary acceptor A_0 (chlorophyll a) and the secondary acceptor A_1 (phylloquinone). It has been shown that the primary radical pairs $P700^{\bullet+}A_0^{\bullet}$ (or $P700^{\bullet+}I^{\bullet}$) recombine to the triplet state of the donor in all photosynthetic reaction centers.[7] This aspect in PS I is still rarely reflected in artificial photosynthesis except for a few triad systems by Levanon and Wasielewski.[8−10]

Here we show that a dyad, consisting of morpholine (MP) as the donor D and silicon phthalocyanine (SiPc) as the acceptor A,

can also be employed to mimic the formation of local triplet state from CSS in PS I.

In this study, D represents MP moiety (Scheme 1), while A stands for silicon SiPc sub unit. Pc molecules contain a planar π system and can be taken as tetraaza-tetrabenzo zinc porphyrins. They are good electron acceptors and frequently selected in artificial photosynthesis for several advantages, as shown by other researchers[11−17] and us:[18−24] (1) strong absorbing ($\varepsilon_{max} \approx 3.0 \times 10^5$ M^{-1} cm^{-1}) in the region of 600−800 nm where solar emission is the richest that reaches the earth surface,[25] many model systems with small π-chromophores that are good for mechanism study are not actually competitive to the silicon solar cell, because they are not absorbing in the red region; (2) excellent stability to heat and light which is extremely important for the long lasting commercial use; (3) easy preparation with low cost starting materials;[26] (4) redox properties and spectral characterization of anion radicals have been understood extensively.[27,28] Pc complexes are therefore quite possible to be practically utilized in the artificial photosynthetic systems. Hence evaluating the role of T_1 state of Pc in PET is important and also the purpose of this study.

The donor moiety in our study is morpholine, which is commercially available. Morpholine-based compounds have been widely studied for their pharmacological properties, for example, as an antipsychotic drug, radiosensitizer, and antifungal drug. This heterocycle features both amine and ether functional groups, hence functions as good electron donors.

Scheme 1. Synthesis of MP$_2$−SiPc

Cl$_2$-SiPc   MP$_2$-SiPc
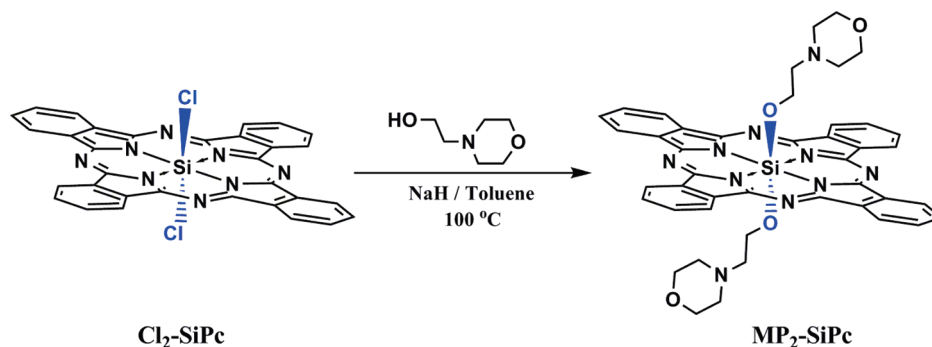
■ EXPERIMENTAL SECTION

Generation Information. All organic solvents were dried by appropriate methods and distilled before use. Cl$_2$−SiPc was purchased from Sigma-Aldrich. All other reagents were analytical grade and used as received. ^{1}H NMR spectra were recorded at roomtemperature on a Bruker dmx 300 MHz NMR spectrometer. MS spectra were recorded either on a Bruker APEX II or Autoflex III Maldi-TOF spectrometer. IR spectra were recorded at room temperature on a Shimadzu FTIR-8900 spectrometer. Samples for C, H, N elemental analysis were dried under vacuum, and analyzed with a Carlo Erba-1106 instrument.

Bis(2-morpholinoethoxy)silicon Phthalocyanine (MP$_2$−SiPc).^{29}. In 10 mL of toluene containing 0.061 g (0.10 mmol) of Cl$_2$−SiPc and 0.010 g (0.40 mmol) of NaH, 0.033 g (0.21 mmol) of morpholine was added with stirring. The resulting solution was heated to 100 °C and kept stirring for 7 h. After it was cooled to room temperature, it was filtered and washed with hexane. The dried solid was purified by recrystallization in toluene to give blue needles (50 mg, 63%). Anal. Calcd For C$_{44}$H$_{40}$N$_{10}$O$_4$Si: C, 65.98; H, 5.03; N, 17.49. Found: C, 65.72; H, 5.22; N, 17.23. ^{1}H NMR (CDCl$_3$, δ (ppm)): 9.73−9.70 (m, 8H, Pc−H$_\alpha$), 8.48−8.43 (m, 8H, Pc−H$_\beta$), 2.83−2.55 (m(br.), 8H, NCH$_2$), 0.69−0.45 (m(br.), 8H, OCH$_2$), −0.05 to −0.13 (m, 4H, CH$_2$N), −1.70- (virtual s, 4H, SiOCH$_2$) ppm. MS (ESI): m/z 800.9 (M$^+$). IR (KBr) (ν_{max}, cm^{-1}): 3063, 2883, 2852, 1610, 1521, 1475, 1426, 1333, 1293, 1120, 1082, 913, 736, 570, 532. UV/vis (DMF, λ_{max} (ε, M^{-1} cm^{-1})): 357 (3.3 × 10^4), 606 (2.5 × 10^4), 673 nm (1.6 × 10^5).

Photophysical Measurements. DMF and other solvents were dried and freshly distilled before use. Measurements were carried out at room temperature of 22 °C. UV−vis absorption measurements were made with a Shimadzu 4500 spectrophotometer in 10 mm quartz cuvettes. Fluorescence spectra up to 900 nm were monitored using EI FLS920, with 1 nm slits. All spectra were corrected for the sensitivity of the photomultiplier tube. The fluorescence quantum yield (Φ_f) was calculated by $\Phi_f = F_s A_0 \Phi_f^0/(F_0 A_s)$, in which F is the intergated fluorescence intensity, A is the absorbance at excitation wavelength, the subscript 0 stands for a reference compound and s represensts samples. Zinc phthalocyanine in DMF was used as the reference ($\Phi_f^0 = 0.30$).^{30} Excitation wavelengths of 610 nm corresponding to S$_0$ to S$_1$ transitions were employed. The sample and reference solutions were prepared with the same absorbance (A_i) at the excitation wavelength (near 0.09 per cm). All solutions were air saturated. Fluorescence lifetime of S$_1$ was measured by time-correlated single photon counting method (Edinburgh FLS-920 spectrophotometer) with excitation

at 672 nm by a CdS portable diode laser (50 ps pulse width) and emission was monitored at 690 nm. Transient spectra were recorded in degassed DMF (prepared by bubbling with argon for 20 min) with an Edinburgh LP-920 laser flash photolysis system. A Nd:YAG laser (Brio, 355 nm and 5 ns fwhm) was used as excitation source. The analyzing light was from a xenon lamp. The laser and analyzing light beams perpendicularly passed through a quartz cell with an optical path length of 1 cm. The signal was displayed and recorded on a Tektronix TDS 3012B oscilloscope and an Edinburgh LP920 detector. The laser energy incident at the sample was attenuated to a few millijoules per pulse. Time profiles at a series of wavelengths from which point by-point spectra were assembled were recorded with the aid of a PC controlled kinetic absorption spectrometer. The concentrations of the target compounds were typically 10 μM providing A_{355} = 0.30 in a 10 mm cuvette. The triplet quantum yield Φ_T was obtained by comparing the ΔA_T of the optically matched sample solution at 355 nm in a 1 cm cuvette to that of the reference using the equation^{31}

$$\Phi_T = \Phi_T^{ZnPc} \cdot \frac{\Delta A_T}{\Delta A_T^{ZnPc}} \cdot \frac{\Delta \varepsilon_T^{ZnPc}}{\Delta \varepsilon_T} \qquad (1)$$

where the superscript represents the reference, ΔA_T is the absorbance of the triplet transient difference absorption spectrum at the selected wavelength, and $\Delta \varepsilon_T$ is the triplet state molar absorption coefficient. The triplet−triplet absorption coefficients ($\Delta \varepsilon_T$) of the samples were obtained using the singlet depletion method,^{31} and the following equation was used to calculate the $\Delta \varepsilon_T$.

$$\Delta \varepsilon_T = \varepsilon_S \frac{\Delta A_T}{\Delta A_S} \qquad (2)$$

where ΔA_S and ΔA_T are the absorbance change of the triplet transient difference absorption spectrum at the minimum of the bleaching band and the maximum of the positive band, respectively, and ε_S is the ground-state molar absorption coefficient at the UV−vis absorption band maximum. Both ΔA_S and ΔA_T were obtained from the triplet transient difference absorption spectra.

Electrochemistry. Cyclic voltammetry measurements were performed using Shanghai CHI model CHI610 electrochemical workstation in argon saturated DMF, tetraethyl ammonium perchlorate was used as supporting electrolyte. A conventional three-electrode system was used. The working electrode was glassy carbon (GCE, 3 mm diameter) vs SCE as reference electrode. Platinum wire was used as the counter electrode. The MP$_2$−SiPc concentration is 1.0 mM.

■ RESULTS AND DISCUSSION

PET Based on Static and Dynamic Quenching of Fluorescence. Figure 1 displays the fluorescence emission spectra of MP_2—SiPc and Cl_2—SiPc in DMF recorded under the same condition. The replacement of chlorine by morpholine caused a very significant decrease of fluorescence intensity. The fluorescence quantum yield (Φ_f) of MP_2—SiPc is 0.071, which is only 11.8% for Cl_2—SiPc. A morpholine molecule contains a nitrogen atom attached by three $-CH_2CH_2O-$ groups, which is similar to triethylamine that acts as a good electron donor in PET.

The measurement of fluorescence lifetime, as shown in Figure 2, gives a further support of intramolecular PET. A visual examination of Figure 2 can already tell that a dynamic quenching occurred in MP_2—SiPc. While Cl_2—SiPc exhibits a
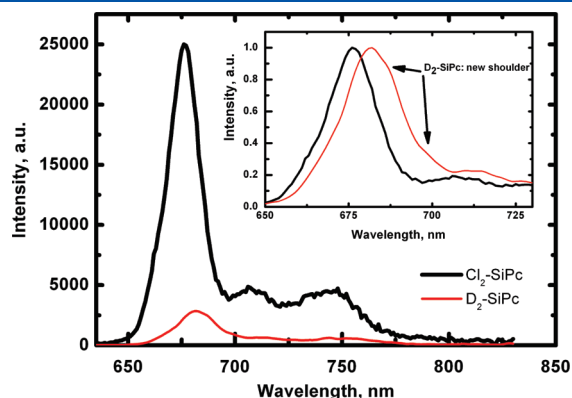

Figure 1. Corrected fluorescence emission spectra of MP_2—SiPc and Cl_2—SiPc in DMF with excitation at 610 nm (absorbance was adjusted to be 0.090). Inset shows their normalized emission spectra.
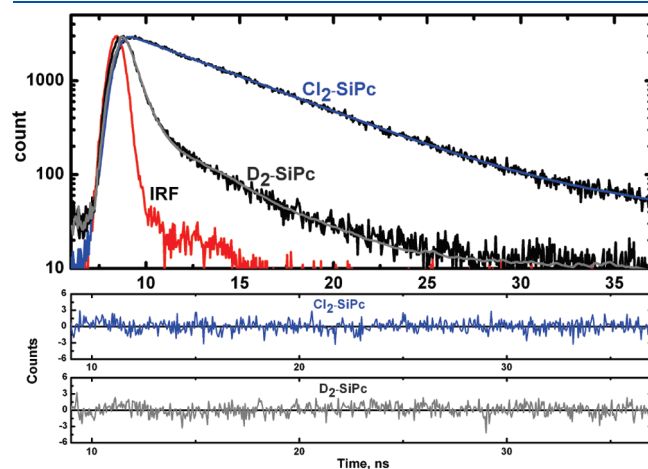

Figure 2. Top: The fluorescence decay curves and fittings of MP_2—SiPc (i.e., D_2—SiPc) and Cl_2—SiPc in DMF with 50 ps laser excitation at 672 nm (the concentration was adjusted to be $\sim$10 μM), the monitored wavelength was 690 nm. Middle and bottom figures show their fitting residue. χ^2 values are listed in Table 1. IRF: instrument response function.

typical monoexponential decay with the fluorescence lifetime (τ_f) of 5.51 ns, MP_2—SiPc shows biexponential behavior. The short-lived component features a τ_f of 0.83 ns, while the long one has a τ_f of 4.77 ns. The τ_f of short-lived emitting species is significantly shortened to 15% of the value for Cl_2—SiPc, due to PET from morpholine moieties to the excited singlet state (S_1) of SiPc subunit.

The influence of solvent polarity on τ_f and Φ_f of MP_2—SiPc was also examined; the results are shown in Table 2 and Figure 3. The decrease of the polarity caused the significant increase of Φ_f from 0.071 in DMF to 0.18 in hexane-toluene mixture (8:1 v/v), which is consistent with the known understanding that PET is more favored by solvents with higher polarity.

MP_2—SiPc is not soluble in pure hexane, so hexane containing small amount of toluene (8:1 v/v) was used. Figure 3 compares the emission decays in different solvents. The decay is biexponential in DMF, but becomes single exponential in hexane-toluene (8:1 v/v). The τ_f of major emitting species is increased from 0.83 ns in DMF, to 4.00 ns in hexane—toluene mixture, which has the same tendency as the Φ_f change upon solvent polarity. This solvent effect clearly supports the presence of PET within MP_2—SiPc. The de-excitation of S_1 often presents biexponential behavior when PET is involved in the process. Two processes are likely responsible for the biexponential nature: (i) CR (charge recombination) emission of CSS:[32,33] $D^{\bullet+}-A^{\bullet-} \rightarrow D-A + h\nu'$, a red-shifted weak emission usually occurs due to the lower energy level of $D^{\bullet+}-A^{\bullet-}$ than $D-^1A$; (ii) the existence of unfavorable conformer for PET in donor—acceptor constructs, no new emission band is expected in this case.[34−36]

To reveal the nature of the minor emitting species, attention was paid to the time-resolved emission spectra, as given in Figure 4. The initially formed emitting species has an emission maximum at 685 nm, which corresponds to S_1 state of SiPc moiety. After 4.0 ns, that is, the short-lived species is almost disappeared, the remained emission spectra showed the emission maximum at 740 nm, indicating the presence of a second emitting species, which is both long-lived and red-shifted. The spectrum of the fast decaying component in Figure 4 shows some difference from the one in Figure 1 because of the error given by the software, which

Table 2. Effect of Solvent on Photophysics of MP_2—SiPc[a]

solvent	Φ_f	τ_1, ns	τ_2, ns	η_2	χ^2	λ_{em}, nm
DMF	0.071					
		0.84	4.77	35.84	1.04	680
		0.85	4.87	35.28	1.06	720
		0.85	4.68	38.24	1.07	740
hexane—toluene (8:1 v/v)	0.18					
		4.03			1.13	680
		3.99			1.11	720
		3.98			1.15	740

[a] τ_1 and τ_2 are obtained from fitting data to $I(t) = A + B_1 e^{(-t/\tau_1)} + B_2 e^{(-t/\tau_2)}$. η_2 is the percentage contribution of second emitting species to fluorescence intensity. λ_{em} is the wavelength at which τ_f is measured.

Table 1. Photophysical Properties in DMF

	λ_{abs}, nm	$lg\varepsilon$	λ_{em}, nm	Stoke's Shift, nm	E_s, eV	Φ_f	τ_f, ns	χ^2	k_f, 10^9 s^{-1}	k_{et}, 10^9 s^{-1}	Φ_T
Cl_2—SiPc	668	5.4	676	8	1.85	0.60	5.51	1.14	0.11	n.a.	0.35
MP_2—SiPc	673	5.2	682	9	1.83	0.071	0.83, 4.77	1.04	0.090	1.02	0.30

8599

dx.doi.org/10.1021/jp202997e |*J. Phys. Chem. A* 2011, 115, 8597–8603
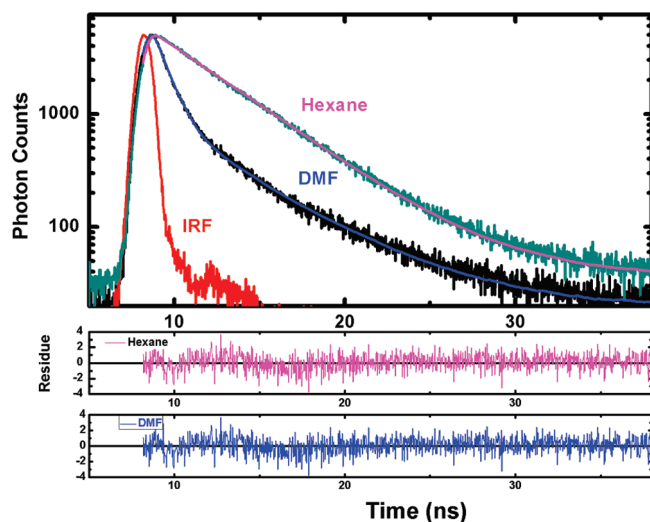
Figure 3. Effect of solvent on fluorescence decay of MP$_2$−SiPc (i.e., D$_2$−SiPc) with 50 ps laser excitation at 672 nm (the concentration was adjusted to be ∼10 μM), the monitored wavelength was 680 nm. The bottom figures show their fitting residue. χ^2 values are listed in Table 2. IRF: instrument response function. The solvent hexane contains 11% toluene.
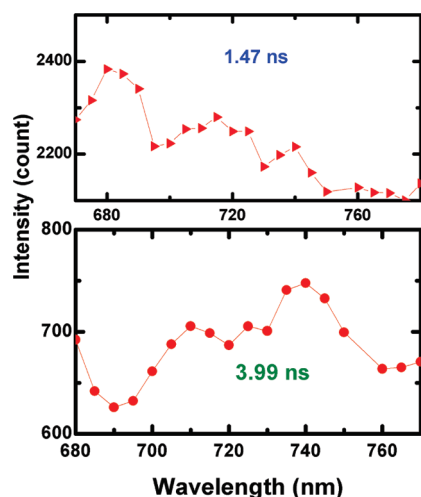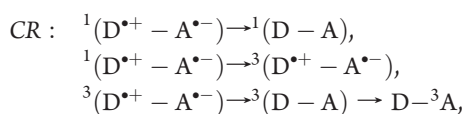

Figure 4. Time-resolved emission spectra of MP$_2$−SiPc in DMF at 1.47 and 3.99 ns with excitation by 50 ps laser at 379 nm (the concentration was adjusted to be ca. 10 μM).

ignores the instrument response when calculating the time-resolved emission spectra.

Since $^1(D^{\bullet+}−A^{\bullet−})$ may undergo several decay processes below as revealed later, including

$$CR: \quad ^1(D^{\bullet+} − A^{\bullet−}) \rightarrow {}^1(D − A),$$
$$^1(D^{\bullet+} − A^{\bullet−}) \rightarrow {}^3(D^{\bullet+} − A^{\bullet−}),$$
$$^3(D^{\bullet+} − A^{\bullet−}) \rightarrow {}^3(D − A) \rightarrow D − {}^3A,$$

in which A = SiPc and D = morpholine.

The latter two processes may also be involved in emitting photons contributing to the long-lived emission.

As shown in Figure 5, MP$_2$−SiPc shows almost exactly the same band shape as that of Cl$_2$−SiPc except for a slight red shift. This close similarity between the two absorptions suggests that
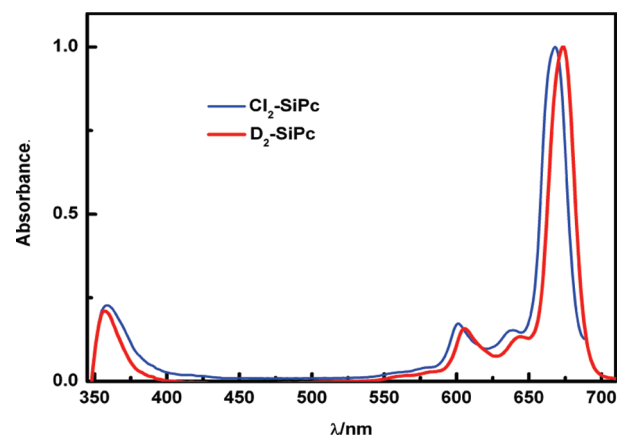

Figure 5. Normalized UV−vis absorption spectra of Cl$_2$−SiPc and MP$_2$−SiPc (i.e., D$_2$-SiPc) in DMF.

the ground state electronic coupling between D and A is fairly weak, although the excited state S$_1$ of A is strongly quenched by the donor D. The quantum yield of CR emission ($\Phi_{f,CR}=\Phi_f\eta_2$) is 0.071 × 35%, which is 0.025.

Thermodynamic analysis provides us with more firmed evidence that PET can occur while thermal (i.e., ground state) electron transfer is forbidden.

Thermodynamics of PET. In cyclic voltammetry of MP$_2$−SiPc, the half wave reduction potential of SiPc moiety is $E_{(SiPc\bullet−/SiPc)}$ = −0.85 V in DMF, smaller than −0.96 V of Cl$_2$−SiPc,[27] while the oxidation of MP moiety is $E_{(MP/MP\bullet+)}$ = 0.86 V, similar to the 0.87 V reported.[37]

The electron transfer from MP to SiPc moiety in their ground states is not thermodynamically allowed, due to the large positive value of free energy change (ΔG) calculated by $\Delta G_{ET} = E_{ox} − E_{red} − C = 0.86 − (−0.85) − 0.06 = 1.65$ eV, in which E_{ox} is the oxidation potential of a donor, E_{red} represents the reduction potential of an acceptor, and C is a small constant associated with solvent, which was evaluated by $−e^2/(r\varepsilon)$ (ε is the permittivity of medium, r is the edge distance between D and A, and e is the electronic charge).

PET from MP to S$_1$ of SiPc moiety (by the photo excitation of the Pc moiety), on the other hand, is thermodynamically favored, since its ΔG is a negative value obtained by: $\Delta G_{PET} = \Delta G_{ET} − E_{00}$ (SiPc) = 1.65 − 1.83 = −0.18 eV.

The T$_1$ energy of SiPc moiety in MP$_2$−SiPc is not expected to varied significantly from 1.0 eV of SiPc,[31] since the maxima of absorption, excitation and emission spectra are not altered remarkably. PET from MP donors to T$_1$ of SiPc moiety is also forbidden, since the energy of the T$_1$ state (∼1.0 eV), which is fairly low and suggesting a ΔG of +0.65 eV.

Energy transfer from SiPc to MP is not possible, since MP does not absorb photons in visible region.

Efficiency and Kinetics of PET. The rate constant of PET (k_{et}) in DMF can be calculated from the fluorescence lifetime data using eq 3, in which τ_0 is the fluorescence lifetime of Cl$_2$−SiPc, while τ_1 is the value of short-lived component for MP$_2$−SiPc. k_{et} is thus obtained as 1.02 × 10^9 s$^{−1}$ in MP$_2$−SiPc.

$$k_{et} = \tau_1^{−1} − \tau_0^{−1} \tag{3}$$

Efficiency for PET (Φ_{et}) was calculated to be 85% by using the k_{et} value ($\Phi_{et} = k_{et}\tau_1$), which indicates that PET is efficient in the system. k_f (the rate constant of fluorescence emission from S$_1$,

8600

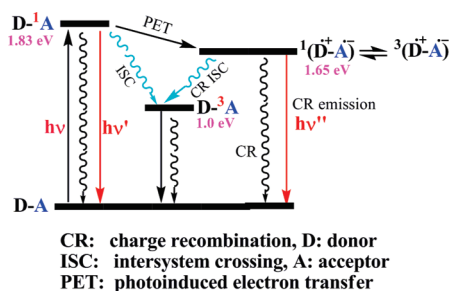dx.doi.org/10.1021/jp202997e |*J. Phys. Chem. A* 2011, 115, 8597–8603

Figure 6. Kinetic scheme for the photophysical process in MP$_2$–A.

Figure 7. Transient absorption spectra in degassed DMF with laser excitation at 355 nm (both absorbance were adjusted to be the same at 0.30), laser energy was the same for both compounds and reduced to 1.0 mJ to avoid triplet–triplet annihilation. Inset shows the decays at 490 nm.

computed by $k_f = \Phi_f/\tau_f$) is 0.11×10^9 s^{-1} for Cl$_2$–SiPc and 0.90×10^8 s^{-1} for MP$_2$–SiPc, respectively, showing that only minor change of k_f occurs upon the introduction of morpholine into SiPc. This slight decrease in k_f is the result of the larger size of MP than Cl atom, since the rotation of MP moieties can disturb the planarity and rigity of the SiPc π system, both of which disfavor the radiation process. k_{isc} of Cl$_2$–SiPc is 0.64×10^8 s^{-1} ($k_{isc} = \Phi_{isc}/\tau_f$). Apparently, the rate constant of PET (k_{et}) in MP$_2$–SiPc is much larger than its k_f and k_{isc}.

The efficiency of triplet formation of SiPc unit within MP$_2$–SiPc shall be significantly decreased from 35% of Cl$_2$–SiPc to 5.3%, if all T$_1$ is originated from S$_1$ through ISC ($\Phi_{isc} = k_{isc}\tau_f = 0.053$).

The efficiency of CR emission from CSS ($\Phi_{f,CR} =$ (observed $\Phi_{f,CR})/(\Phi_{PET})$ is $0.025/0.85 = 0.030$. On the other hand, $\Phi_{f,CR} = k_{F'}\tau_{CR}$, in which $k_{F'}$ is the rate constant of CR emission, τ_{CR} is the lifetime of CS state. $k_{F'}$ is then calculated to be $0.030/(4.77 \times 10^{-9}$ s$) = 0.63 \times 10^7$ s^{-1}. The complete photophysics for MP$_2$–SiPc is shown in Figure 6.

Figure 8. Nanosecond-scale transient absorption spectra for MP$_2$– SiPc in degassed DMF with laser excitation at 355 nm (absorbance was adjusted to be the 0.30).

Transient Absorption Spectra. Transient absorption spectra were recorded in argon saturated DMF solutions upon laser excitation at 355 nm. Figure 7 displays the μs-scale spectra for both compounds. Cl$_2$–SiPc exhibited the typical triplet–triplet (T$_1$–T$_n$) transient absorptions with maximum at 480 nm as reported.[25] The fitting of transient decay by monoexponential function gave a lifetime (τ_T) of 116 μs in the absence of air. τ_T is shortened to 0.34 μs in the air saturated solution, which is the typical characteristic of triplet signal due to efficient energy transfer to molecular oxygen.

MP$_2$–SiPc, on the other hand, also showed the typical features of T$_1$–T$_n$ absorption, and the signal is unexpectedly as strong as that of Cl$_2$–SiPc under the same condition. The decay at 490 nm showed a lifetime of 109 μs, which was reduced to 0.30 μs by the presence of air, indicating that the signal is due to the triplet of SiPc moiety. [SiPc]$^{\bullet-}$ signal at 580 and 620 nm formed by PET from MP, on the other hand, is too weak to clearly resolvable in the μs time scale.

The triplet quantum yield (Φ_T) of MP$_2$–SiPc, measured under low laser energy to avoid T$_1$ annihilation of Pc,[38−40] was found to be comparable to that of Cl$_2$–SiPc as shown in Table 1, which is 6-fold higher than the predicted value of 5.3%. As mentioned previously, the predicted Φ_T was estimated by assuming that all T$_1$ is originated from ISC in the presence of fast intramolecular PET. Since 85% of S$_1$ in MP$_2$–SiPc is de-excited by PET that generates CSS, we must conclude that the extra amount of triplet state in MP$_2$–SiPc is from CSS generated by CR process, in addition to the minor 5.3% contribution of ISC from S$_1$ of SiPc, as shown in Figure 6. This is different from Cl$_2$–SiPc, for which all T$_1$ comes from S$_1$ through ISC.

The efficient formation of T$_1$ from CSS in MP$_2$–SiPc also predicts a short-lived CSS, which is supported by the lifetime measurement of CT emission. The long-lived component of fluorescence emission is assigned to CSS, which exhibits a lifetime of 4.77 ns. This short lifetime of D$^{\bullet+}$-A$^{\bullet-}$ in ns scale explains why μs-scale spectra in Figure 7 shows no significant contribution of A$^{\bullet-}$ (i.e., [SiPc]$^{\bullet-}$). The ns scale transient absorption spectra in Figure 8, on the other hand, does show the formation and decay of CSS: D$^{\bullet+}$–A$^{\bullet-}$. At the time of 5 ns after laser excitation, the absorption of transient anion A$^{\bullet-}$ (bands at 580, 620, and 450 nm for [SiPc]$^{\bullet-}$) can be clearly resolved in addition to broad T$_1$ absorptions. While the A$^{\bullet-}$ decayed fast, the broad triplet signal at 480 nm was increased concurrently, indicating

Figure 9. Energy diagram that shows the involvement of triplet formation in the CR of CSS.

Figure 10. Transient absorption spectra in degassed DMF with laser excitation at 355 nm (both absorbance were adjusted to be the same at 0.30), laser energy was the same for both compounds but increased to 10 mJ to observe triplet−triplet annihilation.

that the T_1 was formed from the CSS in MP_2−SiPc. Only triplet signal remained for the time of 20 ns after the laser excitation.

T_1 formation ($SiPc^{\bullet -}$−$MP^{\bullet +} \rightarrow {}^3SiPc$−MP) accounts for 32% of the charge recombination ($(0.30-0.030)/0.85$), and the rate constant of this process, k_T (= 0.32/4.77 ns) is 0.68×10^8 s^{-1}. This T_1 formation process is made possible because the CSS $SiPc^{\bullet -}$−$MP^{\bullet +}$ has a higher energy (1.65 eV) than the triplet state ${}^3SiPc$−MP (1.0 eV), as shown in Figure 9. Levanon and Wasielewski first demonstrated unambiguously in the mid 90s in a donor−acceptor triad that triplet was formed by the recombination of CSS.[8−10] Verhoeven et al. have reported a number of such systems in which T_1 can be formed by CR of CSS.[41−45] Fukuzumi et al. also pointed out the importance of the triplet formation of Pc when triplet energy is lower than the CSS level.[46] The process that emit heat from CSS ($SiPc^{\bullet -}$-$MP^{\bullet +} \rightarrow$ SiPc-MP + heat) accounts for approximately 65% of CR (= 1−0.32−0.030), and the corresponding rate constant k is 0.23×10^9 s^{-1} (= 0.65/2.8 ns).

We have shown that CR of the radical ion pair generates the local triplet state of SiPc. No heavy atom or paramagnetic metal ion is involved in the process. Direct excitation of the SiPc chromophore in MP_2−SiPc is followed by intramolecular electron transfer efficiently which leads to the population of the singlet CSS, the associated ΔG_{PET} is a small negative value, but the electron donor and acceptor are linked by a flexible spacer that is not long but allows the MPs folded easily to get D and A close enough for PET occurring quickly, the time required for charge separation is markedly shorter than that for the local intersystem crossing or emission process. Triplet CSS can not be populated directly by electron transfer from MP to ${}^3SiPc$ moiety, due to the large positive ΔG_{PET} for the triplet electron transfer.

It is suggested that the energy of the radical ion pair relative to the local triplet states is a crucial factor in determining the mechanism by which the diamagnetic reactants are regenerated from the pair.[47] ${}^3SiPc$ is the lowest triplet state of the D−A system and its energy is just below the radical ion pair, so that the decay of CR to ${}^3SiPc$−MP is inevitable. Because of the spin multiplicity, ${}^3SiPc$−MP is expected to come from ${}^3(SiPc^{\bullet -}$−$MP^{\bullet +})$, which cannot be formed from triplet CT because of the associated large and positive ΔG_{PET}. The precursor of ${}^3(SiPc^{\bullet -}$−$MP^{\bullet +})$ must be ${}^1(SiPc^{\bullet -}$−$MP^{\bullet +})$. This result suggests that the singlet and triplet CSS in this system interconvert quickly, which further means that the exchange interaction has relatively small value, as well as the singlet and triplet CSS are sufficiently close in energy to allow rapid, hyperfine-interaction driven interconversion. Two reasons are likely responsible for the facile interconversion between singlet and triplet CSS: (1) the spacer across the three-bond bridge separating D and A is flexible enough to allow SiPc and MP close enough; (2) the electron transfer is from the HOMO of MP to
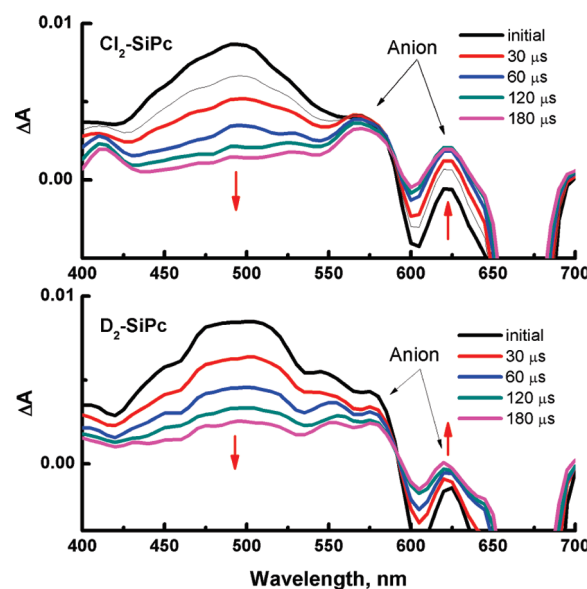
the LUMO of ${}^1SiPc$, whereas the HOMO of MP is the nonbonding orbital of a nitrogen atom (n orbital) and the LUMO is the π orbital, this is basically a n → π* transition. It is known that the intersystem crossing is generally efficient for the excited state because of n → π* transition. Our study on PET in a D−A system, in which SiPc is turned to be the donor while picric acid is the acceptor, is still going on. The preliminary results show that CR of CSS also generates ${}^3SiPc$ but the efficiency is lower, the difference seems mainly because of the large negative free energy when the acceptor was attached to the Pc instead of a donor.

It is worth noting that we need to distinguish $[SiPc]^{\bullet -}$ of PET from $[SiPc]^{\bullet -}$ due to triplet−triplet annihilation. When the laser energy is high enough, as shown in Figure 10, even the μs spectra showed the absorption bands at 580 and 620 nm of $[SiPc]^{\bullet -}$ formed by: $T_1 + T_1 \rightarrow [SiPc]^{\bullet +} + [SiPc]^{\bullet -}$. $[SiPc]^{\bullet +}$ signal at 520 nm is buried in the broad T_1-T_n absorption. One can see that the decay of 480 nm band (for T_1 absorption) is faster than that of the bands at 580 and 620 nm (due to anion $SiPc^{\bullet -}$). Initially T_1 absorption band was higher, but the anion bands became higher after 180 μs. Also the decrease of T_1 absorption was accompanied by the increase of anion absorption, especially at 620 nm, indicating the anion is originated from triplet state.

This $[SiPc]^{\bullet -}$ absorption from T_1 annihilation showed an extremely long lifetime of 581 μs. Other investigations also reported the triplet−triplet annihilation of phthalocyanines.[38−40] We must, however, avoid to assign this long-lived $[SiPc]^{\bullet -}$ to PET process.

■ CONCLUSIONS

Efficient intramolecular PET from morpholine donors to SiPc moiety occurred based on the remarkable efficiency and lifetime quenching of the fluorescence of SiPc subunit by morpholine. The generated charge separation state, $SiPc^{\bullet -}$−$MP^{\bullet +}$ was observable by nanosecond-scale transient absorption spectra. T_1 formation from CSS accounts for 32% of charge recombination: $SiPc^{\bullet -}$−$MP^{\bullet +} \rightarrow {}^3SiPc$−MP, which is made possible by the

8602

dx.doi.org/10.1021/jp202997e |*J. Phys. Chem. A* 2011, 115, 8597–8603

higher energy (1.65 eV) of the CSS $SiPc^{\bullet-}-MP^{\bullet+}$ than that of the triplet state ^3SiPc-MP (1.0 eV). Emission from CSS was also observed: $SiPc^{\bullet-}-MP^{\bullet+} \rightarrow SiPc-MP + h\nu'$ (with 2.5% efficiency and $k_f = 0.63 \times 10^7 \text{ s}^{-1}$).

This study shows that the triplet formation in MP_2-SiPc is also an important CR pathway of the CSS when Pc is involved as a donor or an acceptor, which mimic the process in natural photosynthesis. The main driving force to get local triplet state populated is due to the lower energy of the triplet state, the bridge flexibility and the nature of $n-\pi^*$ interaction between MP and S_1 of SiPc also likely play roles. This triplet formation, on the other hand, may also cause the confusion on PET studies, since T_1-T_1 annihilation upon high laser energy also induces the formation of another long CSS which is easily mistaken as the long-lived CSS formed by PET involving S_1 state.

■ AUTHOR INFORMATION

Corresponding Author

*E-mail: zhangxianfu@tsinghua.org.cn.

■ ACKNOWLEDGMENT

■ REFERENCES

(1) Crabtree, G. W.; Lewis, N. S. *Phys. Today* **2007**, *60*, 37.

(2) Lewis, N. S.; Nocera, D. G. *Proc. Natl. Acad. Sci. U.S.A.* **2006**, *103*, 15729.

(3) Gust, D.; Moore, T. A.; Moore, A. L. *Acc. Chem. Res.* **2009**, *42*, 1890.

(4) Wasielewski, M. R. *Acc. Chem. Res.* **2009**, *42*, 1910.

(5) Fukuzumi, S. *Phys. Chem. Chem. Phys.* **2008**, *10*, 2283.

(6) Araki, Y.; Ito, O. *J. Photochem. Photobiol. C: Photochem. Rev.* **2008**, *9*, 93.

(7) Polm, M.; Brettel, K. *Biophys. J.* **1998**, *74*, 3173.

(8) Greenfield, S. R.; Svec, W. A.; Wasielewski, M. R.; Hasharoni, K.; Levanon, H. Molecular Triads that Mimic the Spin-Polarized Triplet State in Photosynthetic Reaction Centers. In *Reaction Centers Of Photosynthetic Bacteria: Structure And Dynamics*; Michel-Beyerle, M. E., Ed.; Springer-Verlag: Berlin, 1996; pp 81.

(9) Hasharoni, K.; Levanon, H.; Greenfield, S. R.; Gosztola, D. J.; Svec, W. A.; Wasielewski, M. R. *J. Am. Chem. Soc.* **1995**, *117*, 8055.

(10) Hasharoni, K.; Levanon, H.; Greenfield, S. R.; Gosztola, D. J.; Wasielewski, M. R. *J. Am. Chem. Soc.* **1996**, *118*, 10228.

(11) Lee, C.-H.; Guo, J.; Chen, L. X.; Mandal, B. K. *J. Org. Chem.* **2008**, *73*, 8219.

(12) Ito, F.; Ishibash, Y.; Khan, S. R.; Miyasaka, H.; Kameyama, K.; Morisue, M.; Satake, A.; Ogawa, K.; Kobuke, Y. *J. Phys. Chem. A* **2006**, *110*, 12734.

(13) Yui, T.; Kobayashi, Y.; Yamada, Y.; Yano, K.; Fukushima, Y.; Torimoto, T.; Takagi, K. *ACS Appl. Mater. Interfaces* **2011**, *3*, 931.

(14) Lehtivuori, H.; Kumpulainen, T.; Efimov, A.; Lemmetyinen, H.; Kira, A.; Imahori, H.; Tkachenko, N. V. *J. Phys. Chem. C* **2008**, *112*, 9896.

(15) Jakob, M.; Berg, A.; Rubin, R.; Levanon, H.; Li, K.; Schuster, D. I. *J. Phys. Chem. A* **2009**, *113*, 5846.

(16) Gransson, E.; Boixel, J.; Monnereau, C.; Blart, E.; Pellegrin, Y.; Becker, H.-C.; Hammarstrm, L.; Odobel, F. *Inorg. Chem.* **2010**, *49*, 9823.

(17) Poddutoori, P. K.; Poddutoori, P.; Maiya, B. G.; Prasad, T. K.; Kandrashkin, Y. E.; Vasil'ev, S.; Bruce, D.; Est, A. v. d. *Inorg. Chem.* **2008**, *47*, 7512.

(18) Zhang, X. F.; Cui, X.; Liu, Q.; Zhang, F. *ChemPhysChem* **2008**, *9*, 1514.

(19) Zhang, X. F.; Cui, X.; Liu, Q.; Zhang, F. *Phys. Chem. Chem. Phys.* **2009**, *11*, 3566.

(20) Zhang, X. F.; Di, Y.; Zhang, F. *J. Photochem. Photobiol., A* **2009**, *203*, 216.

(21) Zhang, X. F.; Li, X.; Niu, L.; Sun, L.; Liu, L. *Journal of Fluorescence* **2009**, *19*, 947.

(22) Zhang, X. F.; Xi, Q.; Zhao, J. *J. Mater. Chem.* **2010**, *20*, 6726.

(23) Zhang, X. F.; Zheng, H. *Inorg. Chim. Acta* **2010**, *363*, 2259.

(24) Zhang, X. F.; Zheng, H.; Jin, S.; Wang, R. *Dyes Pigm.* **2010**, *87*, 139.

(25) Ishii, K.; Kobayashi, N. The Photophysical Properties of phthalocyanines and Related Compounds. In *The Porphyrin Handbook*; Kadish, K. M., Guilard, R., Ed.; Academic Press: San Diego, 2003; pp 1.

(26) Mckeown, N. B. The Synthesis of Symmetric Phthalocyanines. In *The Porphyrin Handbook*; Kadish, K. M., Guilard, R., Ed.; Academic Press: San Diego, 2003; pp 61.

(27) L'her, M.; Pondaven, A. Electrochemistry of Phthalocyanines. In *The Porphyrin Handbook*; Kadish, K. M., Guilard, R., Ed.; Academic Press: San Diego, 2003; pp 117.

(28) Mack, J.; Stillman, M. Electronic Structures of Metal Phthalocyanines and Porphyrin Complexes from Analysis of the Uv—visable Absorption and Magnetic Circular Dichroism Spectra and Molecular Orbital Calculations. In *The Porphyrin Handbook*; Kadish, K. M., Guilard, R., Ed.; Academic Press: San Diego, 2003; pp 43.

(29) Zhu, Y.-J.; Huang, J.-D.; Jiang, X.-J.; Sun, J.-C. *Inorg. Chem. Commun.* **2006**, *9*, 473.

(30) Seybold, P. G.; Gouterman, M. *J. Mol. Spectrosc.* **1969**, *31*, 1.

(31) Carmichael, I.; Hug, G. L. *J. Phys. Chem. Ref. Data* **1986**, *15*, 1.

(32) Klimov, V. V. *Photosyn. Res.* **2003**, *76*, 247.

(33) Cser, K.; Vass, I. *Biochim. Biophys. Acta Bioenerg.* **2007**, *1767*, 233.

(34) Shibano, Y.; Sasaki, M.; Tsuji, H.; Araki, Y.; Ito, O.; Tamao, K. *J. Organomet. Chem.* **2007**, *692*, 356.

(35) Rubtsov, I. V.; Yoshihara, K. *J. Phys. Chem. A* **1997**, *101*, 6138.

(36) Sakata, Y.; Tsue, H.; O'Neil, M. P.; Wiederrecht, G. P.; Wasielewski, M. R. *J. Am. Chem. Soc.* **1994**, *116*, 6904.

(37) Zhao, Y.; Wasielewski, M. R. *Tetrahedron Lett.* **1999**, *40*, 7047.

(38) Sapunov, V. V. *J. App. Spectrosc.* **2002**, *69*, 831.

(39) Chen, J.; Li, S.; Gong, F.; Yang, Z.; Wang, S.; Xu, H.; Li, Y.; Ma, J. S.; Yang, G. *J. Phys. Chem. C* **2009**, *113*, 11943.

(40) Sapunov, V. V. *Opt. Spectrosc.* **2001**, *91*, 684.

(41) Verhoeven, J. W. *J. Photochem. Photobiol. C* **2006**, *7*, 40.

(42) Hviid, L.; Bouwman, W. G.; Paddon-Row, M. N.; Ramesdonk, H. J.; Verhoeven, J. W.; Brouwer, A. M. *Photochem. Photobiol. Sci.* **2003**, *2*, 995.

(43) Hviid, L.; Brouwer, A. M.; Paddon Row, M. N.; Verhoeven, J. W. *ChemPhysChem* **2001**, *2*, 232.

(44) Roest, M. R.; Oliver, A. M.; Paddon-Row, M. N.; Verhoeven, J. W. *J. Phys. Chem. A* **1997**, *101*, 4867.

(45) van Dijk, S. I.; Groen, C. P.; Hartl, F.; Brouwer, A. M.; Verhoeven, J. W. *J. Am. Chem. Soc.* **1996**, *118*, 8425.

(46) D'Souza, F.; Maligaspe, E.; Ohkubo, K.; Zandler, M. E.; Subbaiyan, N. K.; Fukuzumi, S. *J. Am. Chem. Soc.* **2009**, *131*, 8787.

(47) Roth, H. D.; Schilling, M. L. M. *J. Am. Chem. Soc.* **1980**, *102*, 4303.